Syntheses of $La_{1-x}Ba_xMn_2Al_{10}O_{19}$ Catalysts ($x = 0, 0.05$) in a Novel Microemulsion of Water/2-Propanol/1-Butanol and Their High Activities in Methane Combustion

Fei Teng, Shuhui Liang, Buergen Gauge, and Yongfa Zhu*

Department of Chemistry, Tsinghua University, Beijing 100084, China

Jinguang Xu

Institute of Applied Catalysis, Yantai University, Yantai 264005, China

Guodong Wen, Zhijian Tian, Zheming Wang, Xiaomei Yang, and Guoxing Xiong

State Key Laboratory of Catalysis, Dalian Institute of Chemical Physics, Chinese Academy of Sciences, Dalian 116023, China

Received: February 6, 2007; In Final Form: May 11, 2007

In this work, a novel system of water/2-propanol/1-butanol (W/iP/nB) was developed to synthesize $La_{1-x}Ba_xMn_2Al_{10}O_{19}$ ($x = 0, 0.05$) catalysts. These catalysts were also synthesized by the hydrolysis of the alkoxides in distilled water. The physicochemical properties of the catalysts were characterized by transmission electron microscopy, X-ray powder diffraction, and N_2 adsorption isotherm measurements. The effects of the reaction medium and drying method on the properties of the catalysts were investigated. The results showed that $La_{0.95}Ba_{0.05}Mn_2Al_{10}O_{19}$ catalyst synthesized in W/iP/nB had a higher activity in methane combustion ($T_{10\%} = 425$ °C; $T_{10\%}$ = the temperature at 10% methane conversion) than that prepared in distilled water ($T_{10\%} = 515$ °C). After the reaction was run at 700 °C for 100 h under the reaction conditions, $La_{0.95}Ba_{0.05}Mn_2Al_{10}O_{19}$ catalyst synthesized in W/iP/nB showed a higher stability than that prepared in distilled water. The $LaMn_2Al_{10}O_{19}$ synthesized by subcritical drying showed a higher activity ($T_{10\%} = 440$ °C) than that prepared by conventional oven drying. $La_{0.95}Ba_{0.05}Mn_2Al_{10}O_{19}$ catalyst showed a higher activity than $LaMn_2Al_{10}O_{19}$, which was ascribed to the partial substitution of Ba for La. Furthermore, the structure property of water in W/iP/nB was investigated by means of FT-IR, NMR, electric conductivity, and laser light scattering granulometry. It was proposed that a novel reverse microemulsion of W/iP/nB is formed by distilled water, 2-propanol, and 1-butanol. The hydrolysis of the alkoxides in W/iP/nB was controlled efficiently, just as in a conventional reverse microemulsion.

1. Introduction

Recently, catalytic combustion has attracted great interest due to the high combustion efficiency and extremely low levels of NO_x emissions.[1] The noble metals and perovskite-type oxides are known to be active oxidation catalysts. However, these catalysts are easy to sinter at high temperatures, and this limits their applications in high-temperature combustion of natural gas. Therefore, the synthesis of the catalysts with high thermal stability and high activity is still a challenge to the researchers. Recently, hexaaluminates have attracted particular attention by researchers.[2] Arai et al.[3] have synthesized transitional-metal-substituted barium hexaaluminates with large surface areas and high activities using a sol−gel method. J. Y. Ying et al. have synthesized nanostructured $BaAl_{12}O_{19}$ and $Ce/BaAl_{12}O_{19}$ by a reverse microemulsion method, which have high surface areas and activities of methane combustion.[4] For this microemulsion synthesis, the used surfactant is expensive, and the washing and recovery of the products are laborious. Therefore, the preparation is tedious and expensive, which limits the practical applications in the preparation of the catalyst.

In this work, $La_{1-x}Ba_xMn_2Al_{10}O_{19}$ catalysts ($x = 0, 0.05$) were synthesized in a novel microemulsion of water/2-propanol/1-butanol (W/iP/nB), and the effects of the reaction medium and drying method on the catalysts were investigated. Their catalytic activities in methane combustion were evaluated. Compared with a conventional microemulsion synthesis, this preparation is simpler since the used chemicals are inexpensive and the recovery of the product is easy. Most importantly, the novel W/iP/nB system could also be reused potentially for the preparation of catalysts by supplementing water.

2. Experimental Section

2.1. Preparation of the Catalysts. The used system was composed of distilled water (W), 2-propanol (iP), and 1-butanol (nB). To prepare W/iP/nB, 5−20 mL of water, 5−20 mL of 2-propanol, and 60−90 mL of 1-butanol were mixed and then stirred until the mixture became transparent. Here, V is the volume fraction of water in the system, i.e., $V = V_w/(V_w + V_{iP} + V_{nB})$, in which V_W, V_{iP}, and V_{nB} represent the volumes of distilled water, 2-propanol, and 1-butanol, respectively.

$La_{1-x}Ba_xMn_2Al_{10}O_{19}$ catalysts ($x = 0, 0.05$) were synthesized by the hydrolysis of $Ba(iso\text{-}OPr)_2$ and $Al(iso\text{-}OPr)_3$ in W/iP/nB, which consisted of iP, nB, and an aqueous mixture solution

* To whom correspondence should be addressed. Phone/fax: +86-10-62787601. E-mail: zhuyf@mail.tsinghua.edu.cn.

10.1021/jp071034x CCC: $37.00
Published on Web 06/30/2007

of stoichiometric $La(NO_3)_3$ and $Mn(NO_3)_2$ (W). In a typical procedure, the volume ratio of W to iP to nB was kept at 12.5:12.5:37.5. The stoichiometric $Al(iso\text{-}OPr)_3$ and $Ba(iso\text{-}OPr)_2$ were dissolved in 2-propanol, and the alkoxide solution was dropwise added to the W/iP/nB system to hydrolyze and polycondense, in which the ratio of the alkoxides to water was 1:100 (mole ratio) ($M(OR)_x$, RO = iso-OPr, M = Ba, Al). After being aged for 24 h, the mixture was directly transferred into an autoclave to remove the solvents by subcritical drying (SCD). After the system was maintained at 290 °C and 6.0 MPa for 2 h, the solvents were released slowly at 290 °C. The dried precursor was calcined at 1200 °C for 2 h in a muffle under flowing air.

To investigate the effect of the reaction medium on the catalyst, the precursor of $La_{0.95}Ba_{0.05}Mn_2Al_{10}O_{19}$ catalyst was also synthesized in distilled water. The other procedures were similar to the above procedures.

To investigate the effect of the drying method on the catalysts, the precursor of $LaMn_2Al_{10}O_{19}$ catalyst prepared in W/iP/nB was separated into two parts. One part was dried by SCD, and the other part was dried at 110 °C for 24 h in an oven (conventional drying, CD). The other procedures are similar to the above procedures.

2.2. Characterization. X-ray powder diffraction (XRD) patterns of the catalysts were obtained on a Rigaku D/MAX-RB X-ray powder diffractometer with graphite-monochromatozed Cu Kα radiation (λ = 1.54178 Å), operated at 40 kV, 50 mA, and a scanning rate of 5 deg min^{-1}. Nitrogen adsorption analysis was performed on a Micromeritics ASAP2010 gas adsorption analyzer, operated at 77 K. The surface areas of the catalysts were determined by BET (Brunauer−Emmett−Teller) methods. The catalyst morphology was characterized on a JEOL model 200CX transmission electron microscope, using an accelerating voltage of 200 kV. The samples were deposited on a thin amorphous carbon film supported by copper grids. FT-IR spectra of water in the W/iP/nB system were measured on a Bruker EQUINOX 55 FT-IR spectrometer equipped with an MCT detector. Because the O−H stretching vibration band (ν_{O-H}) of water would overlap with those of 2-propanol and 1-butanol, a definite amount of D_2O was added to the W/iP/nB system to obtain the information on the polarization and hydrogen-bonding interaction of water. In the experiment, the volume ratio of D_2O to ^1H_2O was kept at 4 vol %. The O−D stretching vibration band (ν_{O-D}) of D_2O could reflect the structure property of water in the W/iP/nB system.[5] ^1H NMR spectra were taken on a Bruker DRX-400FT nuclear magnetic resonance spectrometer operating at 400 MHz at 25 ± 0.1 °C. Me_4Si (TMS) was dissolved in $CDCl_3$ and used as an external reference substance to determine the chemical shifts of the ^1H spectra. The electric conductivity (EC) of the system was measured with a LEICI model DDS-11A conductometer using a cell with a constant of 1.005 cm^{-1}. The size distribution of the AlOOH colloidal particles (PSD) formed in the W/iP/nB system was measured with a Malvern Zeta Sizer 1000 laser light scattering granulometer.

2.3. Combustion of Methane. The combustion reaction of methane was conducted in a conventional flow system under atmospheric pressure. A 1 mL (~1.1 g) portion of the catalyst was diluted with 2 mL of quartz powder and loaded into a quartz reactor (i.d. 10 mm), with quartz powder packed at both ends of the catalyst bed. A mixed gas of methane (2 vol %) and air (98 vol %) was fed into the catalyst bed at a gas hourly space velocity (GHSV) of 48 000 h^{-1}. The compositions of the inlet and outlet gases were analyzed with an on-line gas chromatograph with a packed column of carbon molecular sieves and a thermal conductivity detector (TCD). To investigate the stability of the catalyst, the reaction was maintained at 700 °C for 100 h under the reaction conditions. The conversion of methane was measured every 4 h.

TABLE 1: Effect of the Compositions of the Reaction Medium on the Surface Area of $La_{0.95}Ba_{0.05}Mn_2Al_{10}O_{19}$ Catalyst

catalyst no.	W:iP[a]	W:nB[a]	SA[b] ($m^2\ g^{-1}$)
LBMA-1	1:1	1:1	32.4
LBMA-2	1:1	1:2	41.1
LBMA-3	1:1	1:3	51.7
LBMA-4	1:3	1:1	28.3
LBMA-5	1:4	1:1	25.1
LBMA-6	1:5	1:1	24.9
LBMA-7	1:0	1:1	19.6
LBMA-8	1:1	1:0	23.3
LBMA-9[c]			24.5

[a] Preparation: $M(OR)_x$:water = 1:100 (mole ratio), W:iP = the volume ratio of water to 2-propanol, W:nB = the volume ratio of water to 1-butanol. [b] SA = surface area calculated by the BET method. [c] LBMA-9 was synthesized in distilled water. All the samples were dried under subcritical conditions (290 °C, 6 MPa) and then calcined at 1200 °C for 2 h.

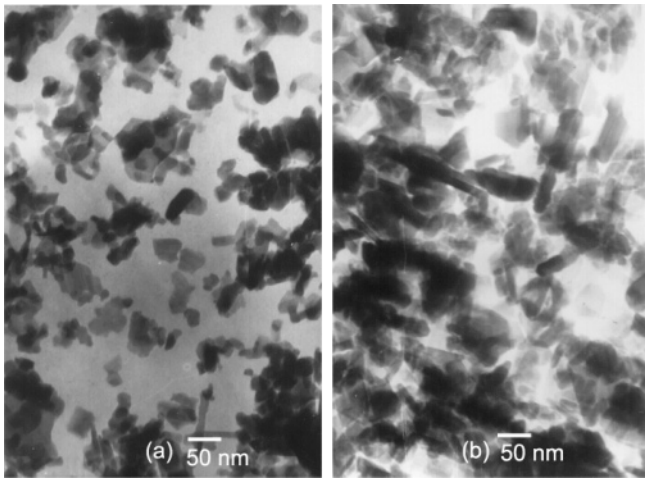

Figure 1. TEM images of $La_{0.95}Ba_{0.05}Mn_2Al_{10}O_{19}$ catalysts prepared in different systems by SCD: (a) W/iP/nB (12.5:12.5:37.5 volume ratio), (b) distilled water [SCD = subcritical drying, W = distilled water, iP = 2-propanol, nB = 1-butanol, $M(OR)_x$:water = 1:100 (mole ratio) (M = Ba, Al, RO = i-PrO)].

3. Results and Discussion

3.1. Syntheses of $La_{1-x}Ba_xMn_2Al_{10}O_{19}$ (x = 0, 0.05) Catalysts. *3.1.1. Effect of the Compositions of the Reaction Medium on the Properties of the Catalysts.* Table 1 gives the effect of the reaction medium on the BET surface area of $La_{0.95}Ba_{0.05}Mn_2Al_{10}O_{19}$ catalyst. Without addition of iP or nB, LMBA-7 and LMBA-8 catalysts had low surface areas (19.6 and 23.3 $m^2\ g^{-1}$, respectively), and LMBA-9 prepared in distilled water had a low surface area of 24.5 $m^2\ g^{-1}$. At W:iP:nB = 1:1:3 (volume ratio), LMBA-3 had the highest surface area of 51.7 $m^2\ g^{-1}$. It is obvious that the compositions of the reaction medium had a significant effect on the surface area of the catalyst. In the studies, the catalysts prepared in W/iP/nB and in distilled water were mainly investigated. LMBA-3 and LMBA-9 catalysts were characterized by transmission electron microscopy (TEM) and XRD. Figure 1 gives the typical TEM images of both catalysts. It can be observed that the average

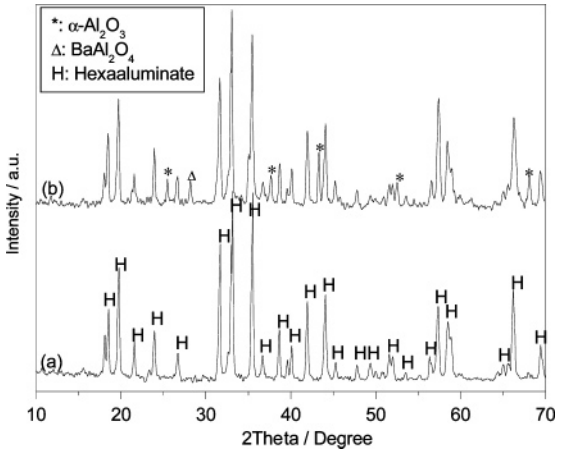

Figure 2. XRD patterns of $La_{0.95}Ba_{0.05}Mn_2Al_{10}O_{19}$ catalysts prepared in different systems by SCD: (a) W/iP/nB (12.5:12.5:37.5 volume ratio), (b) distilled water.

size of $La_{0.95}Ba_{0.05}Mn_2Al_{10}O_{19}$ catalyst synthesized in W/iP/nB is 30 nm, smaller than that (ca. 100 nm) in distilled water. Figure 2 shows their XRD patterns. It can be observed that the synthesized $La_{0.95}Ba_{0.05}Mn_2Al_{10}O_{19}$ catalyst in W/iP/nB is composed of hexaaluminate crystals, and no other impurity crystals could be discerned. However, the prepared catalyst in distilled water is composed of hexaaluminate crystals and small amounts of α-Al_2O_3 and $BaAl_2O_4$ crystals. The low surface area of the catalyst could result from the sintering of these impurity crystals upon calcination at high temperatures. It is obvious that the compositions of W/iP/nB have a significant effect on the particle size and the phase compositions of the catalyst. Probably, the reaction medium may play a role in the hydrolysis of the alkoxides.

3.1.2. Effect of Drying Method on the Crystallization of the Catalysts. $LaMn_2Al_{10}O_{19}$ catalysts were also prepared in W/iP/nB, and the effect of the drying method on the catalysts was investigated. Figure 3 shows XRD patterns of the catalysts and their precursors, which were dried in subcritical conditions (SCD) and in an oven (CD). After drying, both samples were amorphous and no diffraction peaks of oxides or hydroxides (Al, Mn, and La) could be observed. After calcination at 800 °C, diffraction peaks of perovskite ($LaAlO_3$) and alumina appeared for the sample dried by CD. This sample before calcination is amorphous, which may be related to the low drying temperature (110 °C). This indicates that the mixing homogeneity of the constituents in this sample was low. After calcination at 800 °C, however, the sample dried by SCD still remained amorphous. It seems that SCD is beneficial to maintain the mixing homogeneity of the constituents of the precursor. Under subcritical conditions, the dehydration or condensation of M−OH (M = Ba, Al, Mn, and La) favors formation of a strong gel network of M−O−M,[6] which would limit the migration of the inorganic ions. As a result, aggregations of some constituents may be refrained. On the other hand, solvent properties (such as surface tension, dielectric constant, and diffusivity, etc.) can widely change with pressure and temperature.[7] Due to the significant decrease of the dielectric constant of water, the solubility of inorganic ions in subcritical water may be reduced. While water flowed from the inner parts to the surfaces of the pores, the migrations of the inorganic species could also be reduced. As a result, the constituents are highly dispersed in the sample. Moreover, the surface tension of water decreases significantly under subcritical conditions, which could help to maintain the pores in the gel network. Therefore, the mixed homogeneity of the constituents in the sample was

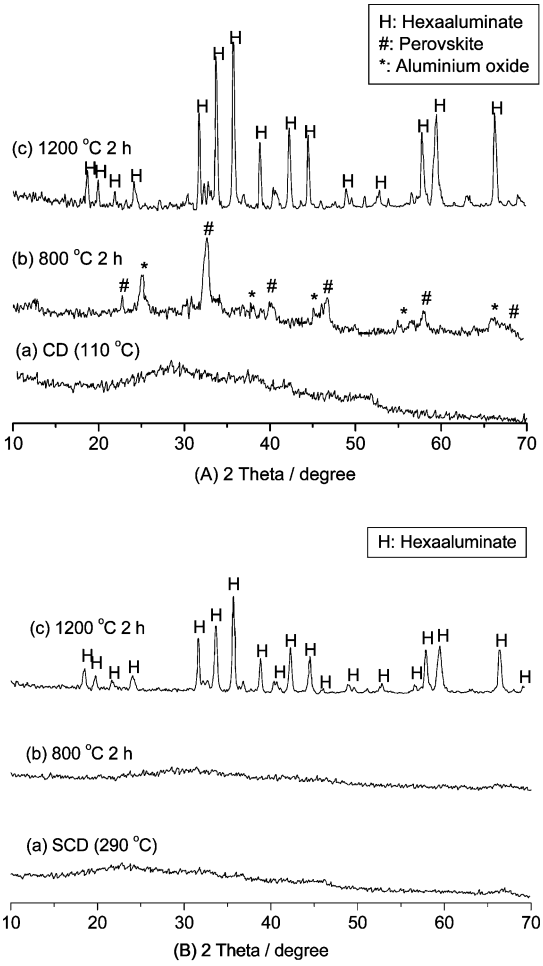

Figure 3. XRD patterns of $LaMn_2Al_{10}O_{19}$ catalysts and their precursors prepared in W/iP/nB by different drying methods: (A) CD, (B) SCD [CD = dried conventionally in an oven, W:iP:nB = 12.5:12.5:37.5 (volume ratio), $Al(OPr)_3$:water = 1:100 (mole ratio)].

maintained after SCD. During the CD process, nevertheless, the pores are easy to crack under the capillary force caused by water with a high surface tension. While the water flowed from the inner parts to the surfaces of the pores, the migrations of some inorganic ions took place. As a result, the mixing homogeneity of the constituents in the precursor was lowered. After calcination at 800 °C, impurity crystals formed. After calcination at 1200 °C, hexaaluminate crystals formed. For both samples, however, it seems that the formation of hexaaluminate crystals proceeded by different phase transformation pathways. For the sample dried by SCD, the hexaaluminate crystals formed directly from the amorphous precursor. Our previous study[8] has shown that the homogeneity of the precursor had a significant influence on the formation of barium hexaaluminate. The high homogeneity of the precursor can favor reactions among Ba, Mn, and Al, because diffusion and rearrangement of the ions could be promoted.[9] As a result, the homogeneous precursor dried by SCD is beneficial to the formation of hexaaluminate crystals. For the sample dried by CD, α-Al_2O_3 and $LaAlO_3$ crystals had formed before the formation of hexaaluminate crystals. The formation of hexaaluminate crystals may proceed via a solid-state reaction (1).[10] The crystallization of hexaaluminate is not easy in this case. Observed from Figure 3, the impurity crystals are still present after calcination at 1200 °C,

$$LaAlO_3 + MnO + Al_2O_3 \rightarrow LaMn_2Al_{10}O_{19} \qquad (1)$$

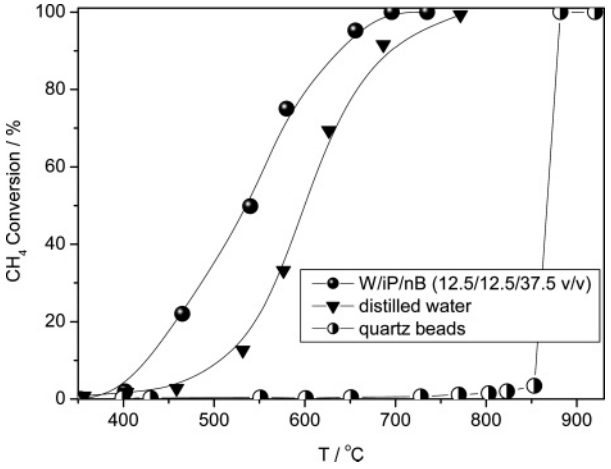

Figure 4. Activities of methane combustion over $La_{0.95}Ba_{0.05}Mn_2Al_{10}O_{19}$ catalysts prepared in different systems by SCD. Reaction conditions: 2% methane, 98% air, GHSV = 48 000 h^{-1}.

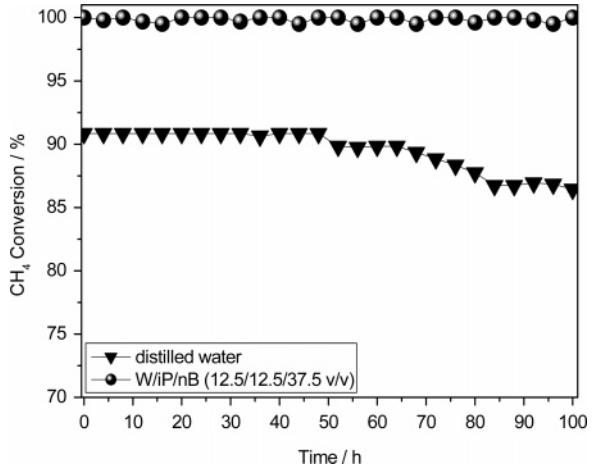

Figure 5. Variations of methane conversion with running time over $La_{0.95}Ba_{0.05}Mn_2Al_{10}O_{19}$ catalysts prepared in diferent systems by SCD. Running conditions: 2% methane, 98% air, GHSV = 48 000 h^{-1}, 700 °C.

and a higher temperature may be needed.[8] This is also supported by the results of Figures S1 and S2 (Supporting Information). Limited by the experimental conditions, the samples were not calcined at temperatures above 1200 °C.

3.1.3. Combustion Activities of Methane over the Catalysts. Figure 4 gives the light-off curves of methane combustion over $La_{0.95}Ba_{0.05}Mn_2Al_{10}O_{19}$ catalyst prepared in different systems by SCD. $T_{10\%}$ (temperature at 10% methane conversion) and $T_{90\%}$ (temperature at 90% methane conversion) over $La_{0.95}Ba_{0.05}Mn_2Al_{10}O_{19}$ catalyst synthesized in W/iP/nB were 425 and 640 °C, respectively, which are much lower than those ($T_{10\%}$ = 515 °C, $T_{90\%}$ = 670 °C) of the catalyst prepared in distilled water. It is well-known that, at low conversions of methane, methane combustion is controlled mainly by surface reaction.[11] Due to its higher surface area (51.7 m^2 g^{-1}), $La_{0.95}Ba_{0.05}Mn_2Al_{10}O_{19}$ catalyst synthesized in W/iP/nB could provide more active sites than that (24.5 m^2 g^{-1}) prepared in distilled water. At high conversions of methane, methane oxidation usually includes surface catalytic reaction and free radical reaction.[11] The free radical reactions are much more dependent on mass transfer than on the surface reaction. Therefore, a low surface area would limit the mass transfer of the reactants and cause the $T_{90\%}$ to be elevated. It is clear that W/iP/nB is superior to pure water for the preparation of the catalysts with high activities, which is also supported by Figure S3 (Supporting Information).

To investigate the stabilities of these catalysts, the lifetime experiments were conducted under the conditions of 2% methane, 98% air, and GHSV = 48 000 h^{-1}. The reaction of methane combustion was run at 700 °C for 100 h, in which significant amounts of water vapor and CO_2 were produced. Figure 5 shows the variations of methane conversion with running time. After the reaction was run for 100 h, the methane conversion over $La_{0.95}Ba_{0.05}Mn_2Al_{10}O_{19}$ catalyst prepared in W/iP/nB did not decrease. However, the methane conversions over the catalyst synthesized in distilled water began to decrease after the reaction was run for 50 h, and the methane conversions decreased from 91% to 85% after the reaction was run for 100 h. The results of N_2 adsorption isotherms showed that, after the reaction was run for 100 h, the surface area of the former was maintained constant (52.2 m^2 g^{-1}), but that of the latter decreased obviously (20.5 m^2 g^{-1}). The different thermal stabilities could be related to their different phase compositions. $La_{0.95}Ba_{0.05}Mn_2Al_{10}O_{19}$ catalyst prepared in W/iP/nB consisted of single-phase hexaaluminate crystals. However, the latter contained small amounts of impurity crystals (α-Al_2O_3 and $BaAl_2O_4$), which are easy to sinter at high temperatures in the presence of water vapor. Therefore, the catalyst synthesized in W/iP/nB had a higher stability than that prepared in distilled water.

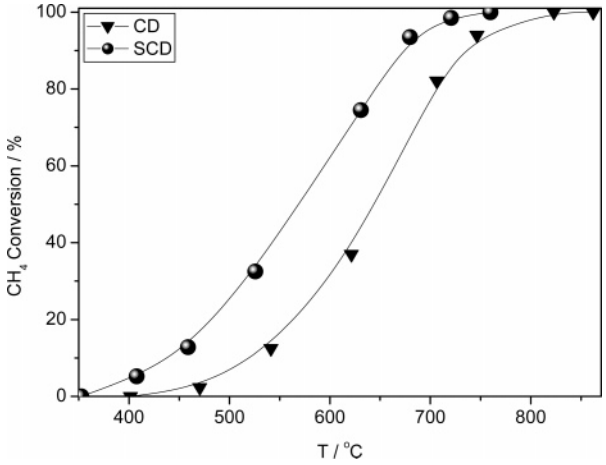

Figure 6. Activities of methane combustion over $LaMn_2Al_{10}O_{19}$ catalysts prepared in W/iP/nB by different drying methods [W:iP:nB = 12.5:12.5:37.5 (volume ratio), Al(Pr-i-O)$_3$/water = 1:100 (mole ratio)]. Evaluation conditions: 2% methane, 98% air, GHSV = 48 000 h^{-1}.

Figure 6 shows the light-off curves of CH_4 combustion over $LaMn_2Al_{10}O_{19}$ catalyst prepared in W/iP/nB by the different drying methods. $LaMn_2Al_{10}O_{19}$ catalyst dried by SCD showed a higher activity ($T_{10\%}$ = 440 °C, $T_{90\%}$ = 670 °C) than that dried by CD ($T_{10\%}$, = 530 °C, $T_{90\%}$ = 760 °C). This is because the former had a higher surface area (53.7 m^2 g^{-1}) than the latter (27.3 m^2 g^{-1}). It is noted that $LaMn_2Al_{10}O_{19}$ catalyst had a lower activity than $La_{0.95}Ba_{0.05}Mn_2Al_{10}O_{19}$ catalyst. Considering their same manganese content and surface area, their different activities may result from the substitution of Ba for La. Although no direct proof was obtained, we could assume that the substitution of bivalent Ba for La would result in unstable oxidation states of manganese (Mn^{3+}/Mn^{4+}). Similar to that of $LaMnO_{3+\lambda}$, the catalytic activity of binary perovskite can further be enhanced by the partial substitution of a bivalent ion for lanthanum.[12−15] Table 2 shows that $La_{0.95}Ba_{0.05}Mn_2Al_{10}O_{19}$ catalyst had the highest reaction rate (intrinsic activity) among the synthesized catalysts. It is obvious that W/iP/nB,

TABLE 2: Surface Area, Reaction Rates, and Activities in Methane Combustion of the As-Prepared Catalysts

catalyst	preparation[a]	SA[b] ($m^2\ g^{-1}$)	$T_{10\%}$[c] (°C)	reaction rate[d] (10^{-5} mol $h^{-1}\ m^{-2}$)
$LaMn_2Al_{10}O_{19}$	W/iP/nB, SCD	53.7	440	8.8
$LaMn_2Al_{10}O_{19}$	W/iP/nB, CD	27.3	530	5.7
$La_{0.95}Ba_{0.05}MnAl_{10}O_{19}$	W/iP/nB, SCD	51.7	425	9.4
$La_{0.95}Ba_{0.05}MnAl_{10}O_{19}$	W, SCD	24.5	515	6.1

[a] Preparation conditions: W/iP/nB (12.5:12.5:37.5, volume ratio), Al(iso-PrO)$_3$:water = 1:100 (mole ratio). SCD = subcritical drying, and CD = conventional drying in an oven. [b] SA = surface area calculated by the BET method. [c] $T_{10\%}$ = temperature at 10% methane conversion. Evaluation conditions of combustion activities: 2% methane, 98% air, GHSV = 48 000 h^{-1}. [d] Measured at 500 °C.

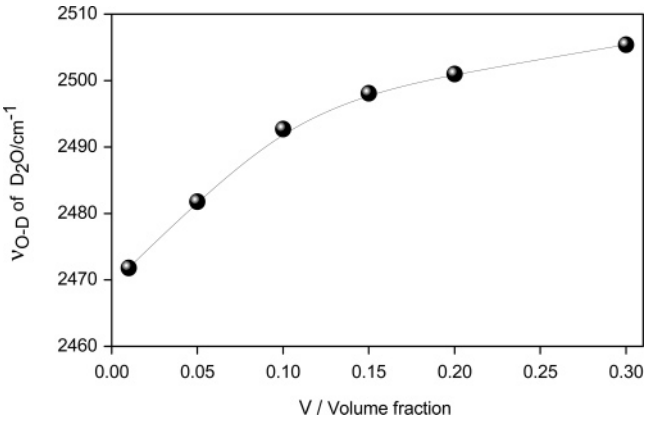

Figure 7. Wavenumber (ν_{O-D}) of the O−D stretching vibration vs the volume fraction (V) of water in the W/iP/nB system (measurement at 25 °C, CaF crystal as the lens, MCT detector).

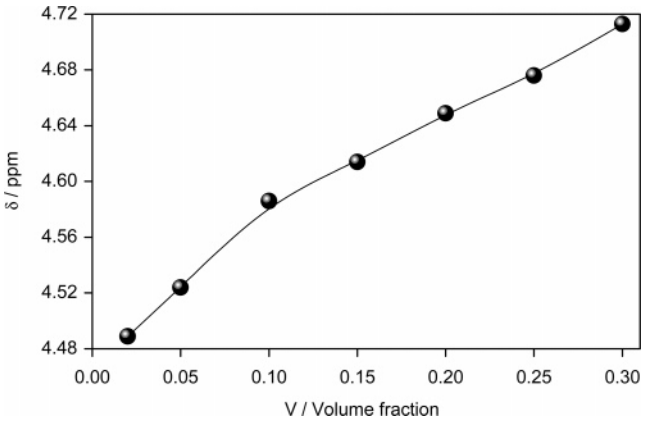

Figure 8. Chemical shift (δ) of ^{1}H NMR against the volume fraction (V) of water in the W/iP/nB system (CaF crystal as the lens, MCT detector).

together with SCD, is useful to obtain catalyst with a high activity. The formation mechanism of the catalysts with high activities in W/iP/nB is not clear yet, and it needs to be investigated further.

3.2. Structure Properties of Water in W/iP/nB. *3.2.1. IR and ^{1}H NMR Spectra*. To understand the structure properties of water in the W/iP/nB system, IR and ^{1}H NMR experiments were conducted. Figure 7 gives the variations of the wavenumber (ν_{O-D}) of the O−D stretching vibration of D_2O with the volume fraction (V) of water in the W/iP/nB system, and the IR spectra of pure water are shown in Figure S4 (Supporting Information). The IR spectra show that the ν_{O-D} bands shift to higher frequencies with increasing V. The blue shift of the ν_{O-D} band indicates that the hydrogen bonds among water molecules become stronger with increasing water content. It has been

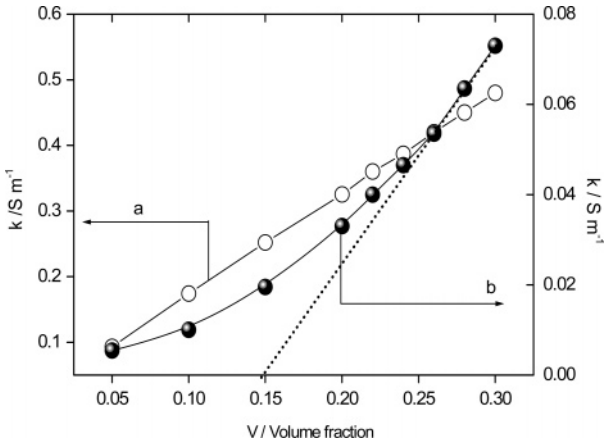

Figure 9. Electric conductivity (κ) vs the volume fraction (V) of a 0.1 M $Mn(NO_3)_2$ aqueous solution in the different systems: (a) 10 mL of distilled water, (b) mixture of 2.5 mL of iP and 7.5 mL of nB.

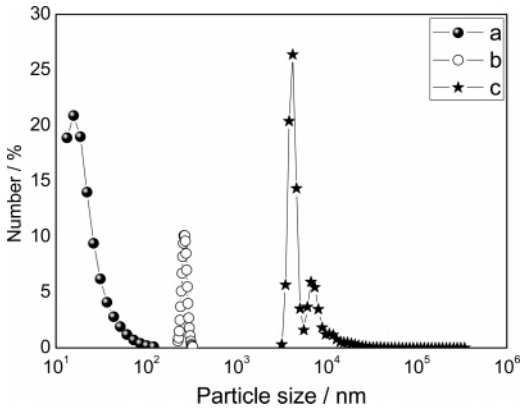

Figure 10. Micelle size of a water/isooctane/1-hexanol/$C_{13}E_6$ (V = 0.05) normal microemulsion (a) and the size distribution of AlOOH colloidal particles prepared in different systems [(b) W/iP/nB (V = 0.125), (c) distilled water] [$C_{13}E_6$ = poly(oxyethylene) (6) tridecane alcohol ether. AlOOH colloidal particles were prepared by the hydrolysis of Al(Pr-i-O)$_3$ [Al(Pr-i-O)$_3$:water = 1:100 (mole ratio)].

reported that ethanol molecules in the nonpolar solvents exist as self-associated aggregates through hydrogen bonds among the ethanol molecules.[16,17] It could be imagined that the hydrogen bonds among water molecules may be gradually disrupted in the presence of iP and nB. Figure 8 shows the ^{1}H chemical shift (δ_{H_2O}) of water in the W/iP/nB system at different water contents. The δ_{H_2O} value represents the electronic microenvironment of ^{1}H of H_2O, which denotes the polarization behavior of water molecules. The larger the δ_{H_2O}, the stronger the polarization and the hydrogen-bonding interactions of the water molecules.[16] At V = 0.02, δ_{H_2O} is ca. 4.49, and δ_{H_2O} gradually shifts to low field with increasing V. This suggests that H-bonds among water molecules become strong with increasing water content in W/iP/nB. Mizuno et al.[18,19] investigated the self-association behavior of ethanol molecules in an aqueous solution by NMR and FT-IR. Their results showed that the self-association of ethanol molecules in an aqueous solution occurs in the whole range of ethanol concentration. Further, hydrogen bonds among water molecules become stronger with an increase of the size of the ethanol aggregates, due to a cooperative effect of the hydrogen bond. Therefore, we could assume that the strengthening of the hydrogen-bonding interactions among water molecules is due to the formation of self-associated water aggregates; the size of the water aggregates, in turn, would increase with the water content (V). From above, it could be held that the small "water aggregates" or "water

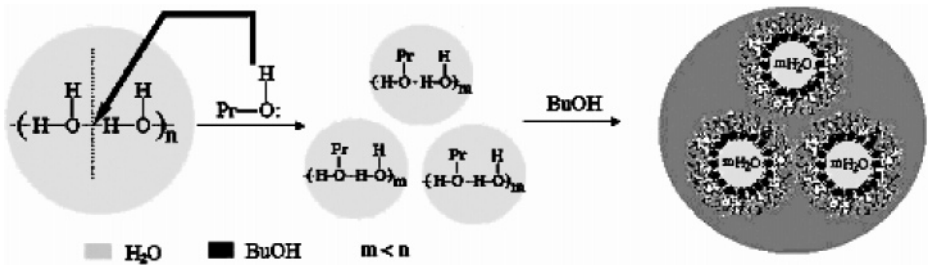

Figure 11. Proposed model of the novel W/iP/nB microemulsion.

clusters" may be formed due to the presence of 2-propanol and 1-butanol molecules.

3.2.2. EC and Laser Light Scattering (LLS). For a conventional nonionic reverse microemulsion, the discrete water droplets and continuous water channels can be easily distinguished by their electric conductivity variations.[20,21] Figure 9 shows the variations of electric conductivity (κ) as a function of the water content in W/iP/nB. An aqueous solution of 0.1 M $Mn(NO_3)_2$, instead of distilled water, was used to increase the electric conductivity of the W/iP/nB system. For the distilled water system, the electric conductivity follows a linear correlation with V. For W/iP/nB, however, the $k-V$ curve is nonlinear when V is low. A critical point of V_0^c (0.15) exists in the $k-V$ curve. As described by Peyrelasse et al.,[22] the conducting behavior of the system could be ascribed to electrophoretic movement of the dispersed water globules when $V \leq V_0^c$. When $V > V_0^c$, the conducting behavior may result from a progressive interlinking or clustering process of water droplets, similar to the conducting behavior of the normal nonionic microemulsion reported by Lagourette et al.[23] The results denote that water aggregates may really be present in the W/iP/nB system.

Laser light scattering technology can be used to measure the size of a water droplet in a conventional reverse microemulsion. Figure 10a shows the size distribution of micelles in the water/isooctane/1-hexanol/$C_{13}E_6$ reverse microemulsion ($V = 0.05$). The sizes of the micelles ranged from 14 to 120 nm. However, we failed in measuring the size distribution of water aggregates in the W/iP/nB system by this method. This may be related to the short lifetime of water aggregates in W/iP/nB, which is not the same as that of the micelles in a normal microemulsion.[24] Zana et al.[25] reported that alcohol aggregates form and break down rapidly. To evaluate the size of the "micelle" of W/iP/nB, AlOOH colloidal particles were prepared by the hydrolysis of Al(Pr-i-O)$_3$ in W/iP/nB ($V = 0.125$) and in distilled water, respectively. The average size of the AlOOH colloidal particles formed in W/iP/nB is 267 nm, as shown in Figure 10b. Generally, the sizes of the colloidal particles formed in a reverse microemulsion are larger than those of micelles acting as nanoreactors.[26,27] Therefore, the average size of the water droplets in the W/iP/nB system would be smaller than 267 nm. However, the average size of the AlOOH colloidal particles formed in distilled water is 5962 nm (Figure 10c), much larger than that (267 nm) of the AlOOH colloidal particles formed in W/iP/nB. By comparison, it seems that the W/iP/nB system is more similar to a conventional reverse microemulsion, rather than distilled water.[28,29]

3.2.3. Proposed Model of the W/iP/nB Reverse Microemulsion. On the basis of the above results, it could be tentatively inferred that a novel reverse microemulsion system may be formed by water, 2-propanol, and 1-butanol. The proposed formation diagram of the novel W/iP/nB microemulsion is shown in Figure 11. In the W/iP/nB system, hydrophilic 2-propanol was used to break hydrogen bonds among water molecules, so that the self-associated water aggregates became smaller; due to the amphiphilic properties of 1-butanol,[30] some 1-butanol molecules acted as surfactants to reduce the surface tension of the water droplets, and most of the 1-butanol molecules acted as a continuous phase. As a result, a novel microemulsion was formed, just as a normal microemulsion. Limited by the experimental conditions, not enough proof has been obtained. Therefore, more studies are still needed.

The most important is that the novel W/iP/nB reverse microemulsion could be used to synthesize the nanoparticles because the hydrolysis and polycondensation of the alkoxides could be controlled effectively by the "reverse micelles".[31,32] In a conventional reverse microemulsion, the used surfactant is generally expensive; it is time-consuming and laborious to recover and wash the solids. All these limit its application in the preparation of the sample. In our W/iP/nB system, inexpensive chemicals are used and the solids are easily recovered from the system. Therefore, under the same drying conditions, the preparation is simpler than the former. Moreover, this novel reverse microemulsion system could be potentially reused for the catalyst preparation by means of supplementing water.

4. Conclusions

A novel reverse microemulsion system was formed with water, hydrophilic 2-propanol, and amphiphilic 1-butanol, and $La_{1-x}Ba_xMn_2Al_{10}O_{19}$ catalysts with high surface areas could be prepared in this novel microemulsion together with subcritical drying. $La_{0.95}Ba_{0.05}Mn_2Al_{10}O_{19}$ catalyst synthesized in this novel microemulsion showed a higher activity in methane combustion ($T_{10\%} = 425$ °C) than the counterpart ($T_{10\%} = 515$ °C) prepared in pure water. $LaMn_2Al_{10}O_{19}$ catalyst prepared in this system by subcritical drying had a higher activity ($T_{10\%} = 440$ °C) than that prepared by oven drying. Due to the partial substitution of Ba for La, $La_{0.95}Ba_{0.05}Mn_2Al_{10}O_{19}$ catalyst showed a higher activity than $LaMn_2Al_{10}O_{19}$ catalyst.

Acknowledgment. We thank the Science and Technology Ministry of China (Grant G1999022401) and Chinese National Science Foundation (Grants 20433010 and 20571047) for financial support.

Supporting Information Available: XRD patterns of $La_{0.95}Ba_{0.05}Mn_2Al_{10}O_{19}$ catalysts dried conventionally in an oven and their activities in methane combustion and IR spectra of pure water. This material is available free of charge via the Internet at http://pubs.acs.org.

References and Notes

(1) Pfefferle, L. D.; Pfefferle, W. C. *Catal. Rev.—Sci. Eng.* **1987**, *29*, 219.

(2) Johansson, E. M.; Danielsson, K. M. J.; Pocoroba, E.; Haralson, E. D.; Jåräs, S. G. *Appl. Catal., A* **1999**, *182*, 199.

(3) Machida, M.; Eguchi, K.; Arai, H. *J. Catal.* **1987**, *103*, 385.

(4) Zarur, A. J.; Ying, J. Y. *Nature* **2000**, *403*, 65.

(5) Zeidler, M. D. In *Water: A Comprehensive Treatise*; Franks, F., Ed.; Plenum Press: New York, 1973; Vol. 2, p 529.
(6) Hayashi, H.; Torii, K. *J. Mater. Chem.* **2002**, *12*, 3671.
(7) Cansell, F.; Chevalier, B.; Demourgues, A.; Etourneau, J.; Even, C.; Garrabos, Y.; Pessey, V.; Petit, S.; Tressaud, T.; Weill, F. *J. Mater. Chem.* **1999**, *9*, 67.
(8) Teng, F.; Xu, P.; Tian, Z.; Xiong, G.; Xu, Y.; Xu Z.; Lin, L. *Green Chem.* **2005**, *7*, 1.
(9) Machida, M.; Eguchi, K.; Arai, H. *Bull. Chem. Soc. Jpn.* **1988**, *12*, 3659.
(10) Machida, M.; Eguchi, K.; Arai, H. *J. Am. Ceram. Soc.* **1998**, *71*, 1142.
(11) Harrison, B. K.; Ernst, W. R. *Combust. Sci. Technol.* **1978,** *19*, 31.
(12) Kosima, I.; Adachi, H.; Yasumori, I. *Surf. Sci.* **1983**, *130*, 50.
(13) Chan, K. S.; Ma, J.; Jaenicke, S.; Chuan, G. K. *Appl. Catal., A* **1994**, *107*, 201.
(14) Jang, B. W-L.; Nelson, R. M.; Spivey, J. J.; Ocal, M.; Oukaci, R.; Marcelin, G. *Catal. Today* **1999**, *47*, 103.
(15) Groppi, G.; Cristiani, C.; Forzatti, P. *Appl. Catal., B* **2000**, *35*, 137.
(16) Leaist, D. *Can. J. Chem.* **1988**, *66*, 1129.
(17) Stokes, R. H. *J. Chem. Soc., Faraday Trans. 1* **1977**, *73*, 1140.
(18) Mizuno, K.; Miyashita, Y.; Shindo, Y. *J. Phys. Chem.* **1995**, *99*, 3225.
(19) Maes, G.; Smets, J. *J. Phys. Chem.* **1993**, *97*, 11134.
(20) Li, Q.; Li, T.; Wu, J. *J. Colloid Interface Sci.* **2001**, *239*, 522.
(21) Teng, F.; Tian, Z.; Xu, J.; Xiong G.; Lin, L. *Stud. Surf. Sci. Catal.* **2004**, *147*, 493.
(22) Peyrelasse, J.; McClean, V. E. R.; Bone, C.; Sheppard R. J.; Clausse, M. *J. Phys. D: Appl. Phys.* **1978**, *11*, L117.
(23) Lagourette, B.; Peyrelasse, J.; Bone, C.; Clausse, M. *Nature* **1979**, *281*, 60.
(24) Osseo-Asare, K.; Arriagada, F. *J. Colloids Surf.* **1990**, *50*, 321.
(25) Zana, R.; Eljebari, M. J. *J. Phys. Chem.* **1993**, *97*, 11134.
(26) Yamauchi, H.; Ishikawa, T.; Kondo, S. *Colloid Surf.* **1989**, *37*, 71.
(27) Bodet, J.-F.; Davis, H. T.; Scriven L. E.; Miller, W. G. *Langmuir* **1998**, *4*, 455.
(28) Guering, P.; Lindman, B. *Langmuir* **1985**, *1*, 464.
(29) Kahlweit, M.; Busse, G.; Jen, J. *J. Phys. Chem.* **1991**, *95*, 5580.
(30) Zana, R.; Michels, B. *J. Phys. Chem.* **1989**, *93*, 2643.
(31) Kilpatrick, P. K.; Davis, H. T.; Scriven, L. E.; Miller, W. G. *J. Phys. Chem.* **1986**, *90*, 5292.
(32) Kahlweit, M.; Strey, R.; Firman, P.; Haase, D. *Langmuir* **1985**, *1*, 281.